Al-Farouk journal of sciences
Volume (2), Issue (4) (Spt, 2026)
ISSN: 3135-2359

مجلة الفاروق للعلوم
المجلد (2) العدد 4 سبتمبر 2026
ردمد: 3135-2359

East-West Coordination and Economic Dispatch of Libya's Power System: Economic Value and Transmission Capacity Sensitivity

Osama Mohammed Abdulrahman [1]* Reyad Al-Farah [2]* Almonir Al-Gnoni [3] * Abdelgani A Mostafa Hussian[4]

ORCID : https://orcid.org/0009-0002-8759-5299 , 0009-0003-7694-7997 , 0009-0008-4666-2014, 0009-0006-2515-579999

Department of Electrical and Electronic Engineering, Faculty of Engineering, Zawiya University, Libya

*Corresponding author: o.abdulrahman@zu.edu.ly; r.elfrah@zu.edy.ly ; a.algnoni@zu.edu.ly ; a.albhlol@zu.edu.ly

Received: 10/9/2026 Revised: 17/9/2026 Accepted: 20/10/2026 Publication: 19/11/2026

Abstract: Independent day-ahead scheduling in interconnected regions can meet the needs of each region, the system-level economic efficiency is low due to the failure to fully utilize the limited exchanges between regions in the scheduling sequence. This paper constructs a 24-hour mixed-integer linear programming model for the Libyan power system to coordinate and optimize unit combination, start-up and shutdown decisions, economic dispatch, and the total east-west exchange variable. Controlled experiments were conducted under three frameworks with the same regional demand, initial state, unit constraints, time constraints, and calibrated cost coefficients: independent scheduling with zero exchange, coordinated scheduling with an exchange limit of 349.6 MW, and a virtually unconstrained mixed baseline. The study is evaluated based on data from 19 authorized operating days starting in 2025, consisting of 25 thermal power plant modules. The MATLAB optimization toolbox provides the main solution, while independent SciPy/ HiGHS reconstructions validate the objective function, completeness, regional balance, ramp-up capability, and minimum time residual. Throughout the sample, coordinated operation reduced the total target capacity from 97.759 million comparative cost units (CUs) to 97.094 million, achieving 86.17% of the combined economic value, reducing the average committed operating units from 9.80 to 9.11, and decreasing the total number of start-ups and shutdowns from 205 to 196. The coordinated operation plan transmitted 105.85 GWh of absolute power and 87.32 GWh of net power from east to west, with model-predicted load shedding at zero. On peak-value days, the target capacity decreased by 1.448%; on peak days of 8166 MW, the decrease was 0.157%. Transmission capacity sensitivity analysis revealed diminishing returns: high-value cases reached saturation near 750 MW, while peak cases achieved almost all available benefits at 500 MW. These results provide a quantitative screening method for prioritizing detailed national grid studies and developing coordinated operation policies.

Keywords: economic dispatch; inter-regional exchange; Libyan power system; mixed-integer linear programming; multi-regional dispatch; unit combination.

1. Introduction

The Libyan power system provides an important application case because its load and generation mix is geographically uneven. The western region has greater demand and installed capacity, while the eastern region, although smaller in mix, can still change the national power dispatch sequence under certain operating conditions. Unit mix (UC) determines which thermal power units are connected to the grid, when to start or stop, and the duration of each operating state. Economic dispatch (ED) allocates hourly demand to the mixed units. These decisions are inextricably linked: unit mix decisions affect available capacity, stable minimum output power, ramping capability and future resilience, while the anticipated dispatch path determines whether starting or stopping a unit is economically justifiable [1]-[7].

When a power system is divided into interconnected regions, local feasibility does not guarantee the overall economic benefits of the system. One region may supply relatively expensive electricity, even if another region has less expensive available power, but such substitution is only feasible if the planned power exchange is still within the capacity range between regions. Therefore, multi-regional coordination requires optimizing power input, dispatch and exchange in a time model [8]-[13].

Forecasting studies in Libya have also confirmed that the country’s electricity demand exhibits significant seasonality and daily operating variation[18]. This study uses official records from Libya’s General Electricity Company (GECOL) to quantify the value of coordinated dispatch[19].

The research questions are clear: When the demand, units, initial state, time constraints, and cost coefficients are the same in the East and West, how much economic and promised value can be obtained by allowing a limited total amount of exchange instead of forcing each region to independently meet its own needs? The second question is: As the exchange limit increases, at what rate will this value reach saturation?

This paper contributes four elements: (1) a transparent two-zone thermal UC-ED formula; (2) a controlled comparison of isolated, coordinated and centralized scheduling; (3) a complete operational-day assessment of target value, exchange direction, commitment depth, transition and technology allocation; and (4) a sensitivity analysis of transfer capability to determine the point of diminishing returns.

Figure 1 outlines the mathematical details introduced into the previous research workflow. It should be read from top to bottom: First, authorized run records are converted to the same regional input; second, the three scheduling frameworks differ only at the exchange boundaries; finally, all results undergo the same feasibility analysis and reporting layer.

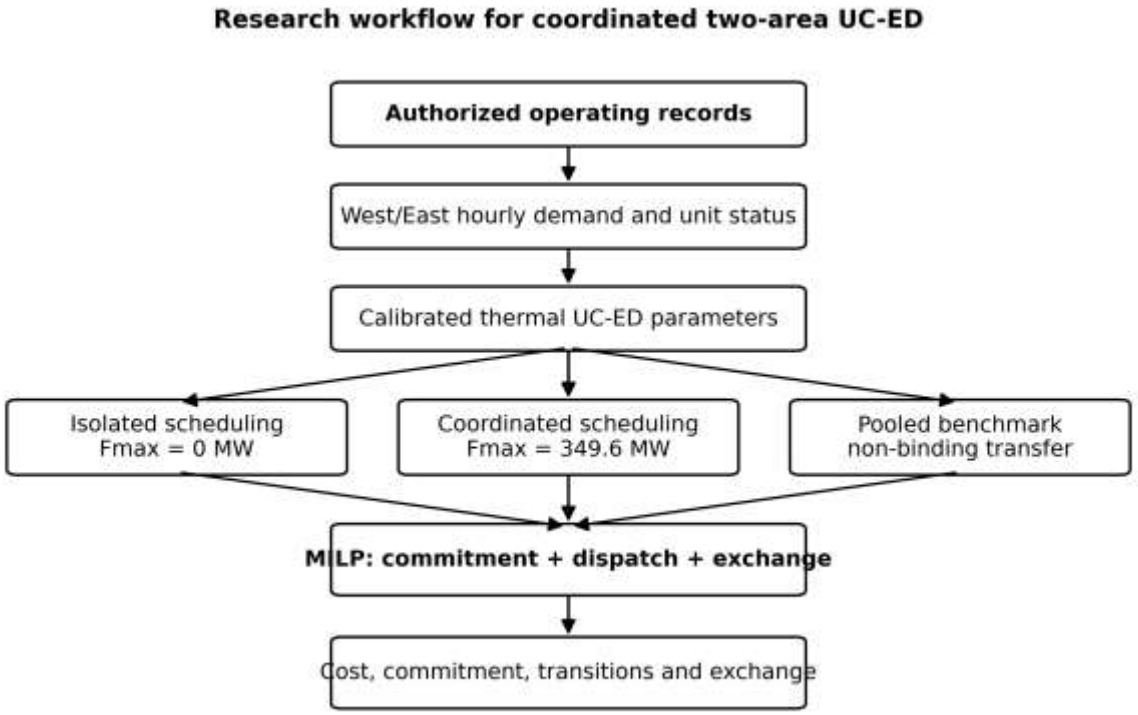


Figure 1. Control study workflow for coordinated dual-region UC-ED.

The separation shown in Figure 1 is crucial for causal explanation. Since the demand, unit data, initial conditions, and time constraints remain constant, the difference in objective value or commitment stems from reconciliation rather than input inconsistency. The remainder of this paper follows the same order: literature review, data presentation, equations, controlled experiments, results, engineering interpretation, and conclusions.

2. Gap between relevant work and research

2.1 Precise UC-ED Formulation

Classical unit combination scheduling methods include priority list, dynamic programming, and Lagrange relaxation. Modern practice increasingly relies on mixed-integer linear programming because binary commitments and continuous scheduling can be represented by an auditable formula [1]-[3]. Rigorous formulation of commitment logic, generation limits, start-up and shutdown ramps, and minimum operating/downtime can improve physical accuracy and solver performance [3]-[6].

Model selection is crucial. Comparative studies have shown that seemingly minor changes in production cost representation, capacity ramp-up, or logical constraints can affect cost, feasibility, and computation time [6][7].

Therefore, this comparative study uses the same entity model in each framework, only changing the exchange capacity.

2.2 Multi-regional coordination

Multi-regional dispatch has long been a combination of factors such as regional commitments, economic dispatch, import and export restrictions and energy-saving allocation[8]. Subsequent studies have extended this issue to situations such as stochastic wind energy uncertainty, decentralized coordination, robust dispatch and competitive market operation[9]-[12]. Reviews of unified dispatch (UC) considering transmission emphasize that dispatch schemes must meet the inter-regional power generation and transmission capacity while ensuring time constraints[13].

The literature has confirmed the importance of coordinated scheduling, but most studies employ standard testing systems or market abstract models. This paper aims to fill this research gap by conducting a controlled experiment focused on Libya, based on official operating records that explicitly disclose total transaction volume and provide complete sensitivity curves, rather than simply assuming a single transfer limit.

2.3 Computational Practice

This study still focuses on the exact mixed integer linear programming (MILP) model. Learning-assisted hot start, feasibility repair and constraint screening can accelerate repeated unit combination (UC) calculations, but these methods are only reliable if the original equations and feasibility tests are still available [14]-[17]. Therefore, this study adopts direct MILP solutions and independent numerical reconstruction, rather than black-box scheduling strategies.

The main innovation lies not in the competition between unrelated solvers, but in providing an economic interpretation of bounded East-West coordination under the same operational evidence and conducting sensitivity analysis to reveal when additional aggregate transfer payments no longer alter the plan.

3. Operational data and dual-region study design

3.1 Authorization Operation Log and Preprocessing

This study used data from 19 authorized operating days throughout 2025 in the GECOL records [19]. Each case included 24-hour national and regional demand observations, power plant generation measurements, and initial operating conditions for establishing a cogeneration dispatch scheme. The selected dates covered winter, spring, summer, and autumn, with system peak power ranging from 4,665 to 8,166 MW.

The preprocessing steps include reconstructing dates and times, distinguishing missing values or non-numerical entries from true zero outputs, standardizing site names, and mapping site observations to a common set of generated blocks. The isolation, harmonization, and aggregation frameworks all use the same preprocessing output. This not only ensures data traceability but also avoids attributing data cleaning discrepancies to the harmonization model.

The optimization scheme comprises 25 site modules. These modules are grouped by region and technology to preserve observed spatial and economic asymmetries while maintaining model transparency. Values not directly provided in the records remain constant across all experiments after a single calibration.

3.2 Dual-region representation

Figure 2 defines the notation conventions and the research boundary. The western and eastern portfolios are represented as aggregated scheduling regions and connected by a controllable exchange variable F_t. A positive

F_t represents a transfer from west to east; a negative F_t represents a transfer from east to west. This figure represents an economic coordination model, not a single-line network model.

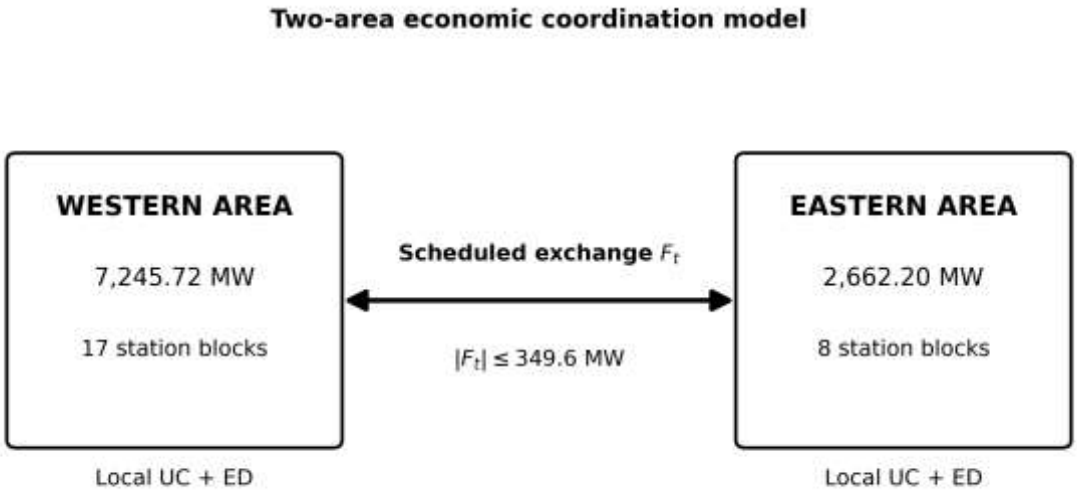


Figure 2. East-West economic coordination model and exchange symbol conventions.

Figure 2 shows that each region retains its own power commitments and dispatch decisions, while the exchange variables are coupled with the regional power balance. The calibrated maximum capacities are 7245.72 MW in the west and 2662.20 MW in the east. The model determines the direction of power exchange hourly, rather than setting permanent power exporting or importing countries.

Table 1 presents three controlled scheduling frameworks. It appears before the portfolio table because the differences in the experiments lie in the exchange boundary, rather than in the changes in generation data.

Table 1. Controlled scheduling framework.

frame	Foreign exchange limit	explain
isolated	0 megawatts	Each region meets its own needs.
coordination	349.6 MW	Combined UC-ED with bounded total quantity exchange.
Summary benchmark	5000 megawatts	It is actually a non-binding exchange used to estimate the value of the available pool of funds.

Table 1 confirms that only the transmission capacity changed. All unit data, loads, initial conditions, cost factors, and time constraints remained constant. The 5000 MW case is not an operational scenario, but a numerical benchmark designed to reveal the maximum economic value achievable by the integrated model employed.

Table 2 describes the regional power generation combinations used in these three architectures. Technology grouping is crucial because coordination mechanisms can replace one technology and region with another while keeping the total power supply constant.

Table 2. Calibrated thermal power generation combinations by region.

area	science and technology	Building Blocks	Calibrate Pmax (MW)
The west	Compound cycle	2	2,025.00
The west	Main gas	7	4,361.04
The west	steam	2	648.00
The west	small gas	6	211.68
East	Compound cycle	2	1,527.12
East	Main gas	3	764.64
East	steam	2	354.24
East	small gas	1	16.20

The asymmetry in Table 2 explains why coordination mechanisms can alter commitments even when Western countries have larger total capacity. Economic substitution depends on regional demand per hour, initial commitments, minimum output, capacity ramp-up capabilities, cycle costs, and limited exchange volumes, not just installed capacity.

Table 3 defines abbreviations and mathematical symbols before their use in formulas. This avoids requiring readers to infer the meaning of symbols from context.

Table 3. Abbreviations and mathematical symbols.

Symbol	definition
University of California	Unit Commitment – Binary Online, Start-up, and Shutdown Decisions.
ED	Economic dispatch – the continuous allocation of active power among committed power segments.
MILP	Mixed-integer linear programming.
CU	Comparison cost unit used for consistent comparisons between models.
us	Western and Eastern dispatch areas.
u_g ,t	The binary online status of block g within hour t.
y_g ,t / z_g ,t	Binary start/stop indicator.
p_g ,t	The active power output (MW) of module g in t hours.
F_t	Total exchange volume; positive for west to east, negative for east to west (MW).
D_ W,t / D_ E,t	West/East hourly demand (megawatts).
s_ W,t / s_ E,t	Non-load reduction diagnostic variables (MW).

4. Mathematical Formulas

4.1 Logic of Goals and Commitments

Let G represent the set of all site blocks, G_W and G_E represent subsets of regions, and T represent the 24-hour interval. The objective function in Equation (1) aims to minimize production costs, idle costs, start-up costs, and downtime costs. A high penalty is imposed on s_n ,t to ensure that load reduction is only performed when infeasibility occurs. This model follows the strong thermal UC structure established in references [2]-[7].

$$\min J = \sum_{t\in\mathcal{T}}\sum_{g\in\mathcal{G}}\left[C_g\left(p_{g,t}\right) + C_g^{NL}u_{g,t} + C_g^{SU}y_{g,t} + C_g^{SD}z_{g,t}\right] + c^{LS}\sum_{n\in\{W,E\}}\sum_{t\in\mathcal{T}}s_{n,t} \quad (1)$$

Formula (2) identifies each online state change as a start or stop. Formula (3) links the binary commitment to the continuous ED: the offline module produces zero output, while the online module remains between the calibrated stable minimum and maximum output.

$$u_{g,t} - u_{g,t-1} = y_{g,t} - z_{g,t} \tag{2}$$

$$P_g^{\min} u_{g,t} \le p_{g,t} \le P_g^{\max} u_{g,t} \tag{3}$$

Formulas (4) and (5) distinguish between the normal ramp-up process and the larger transitions allowed during startup and shutdown. Formulas (6) and (7) guarantee the minimum duration of each operating state. These constraints are crucial in two-region comparisons because seemingly low-cost regional substitutions may not be feasible if the recipient's portfolio cannot change output quickly enough.

$$p_{g,t} - p_{g,t-1} \le RU_g u_{g,t-1} + SU_g y_{g,t} \tag{4}$$

$$p_{g,t-1} - p_{g,t} \le RD_g u_{g,t} + SD_g z_{g,t} \tag{5}$$

$$\sum_{\tau=t-UT_g+1}^{t} y_{g,\tau} \le u_{g,t} \tag{6}$$

$$\sum_{\tau=t-DT_g+1}^{t} z_{g,\tau} \le 1 - u_{g,t} \tag{7}$$

4.2 Regional Power Balance and Exchange

Equations (8) and (9) are the direct integration points between the regional UC-ED and the exchange. According to the notation conventions used, a positive F_t indicates that energy flows from west to east; a negative value indicates that energy flows from east to west. The same F_t value has opposite signs, so the model cannot create or consume energy through exchange.

$$\sum_{g \in \mathcal{G}_W} p_{g,t} + s_{W,t} - F_t = D_{W,t} \tag{8}$$

$$\sum_{g \in \mathcal{G}_E} p_{g,t} + s_{E,t} + F_t = D_{E,t} \tag{9}$$

Formula (10) specifies the aggregated capacity for a specific scenario. Isolated dispatch sets Fmax to zero, coordinated dispatch uses 349.6 MW, and joint baseline dispatch uses 5,000 MW. Hourly power exchanges are economically dispatched within this capacity range.

$$-F^{\max} \le F_t \le F^{\max} \tag{10}$$

4.3 Reporting Indicators

Formula (11) represents the reduction in target cost achieved by coordinated scheduling relative to independent operation. Formula (12) measures how much of the total value of transitioning from independent to shared operation can be obtained from a limited coordinated scheduling scheme. These two indicators answer different questions: the former directly reflects the improvement, while the latter assesses whether the adopted transfer capacity is close to the economic saturation point.

$$S_{coord}(\%) = 100\,\frac{J_{iso} - J_{coord}}{J_{iso}} \tag{11}$$

$$V_{capture}(\%) = 100\,\frac{J_{iso} - J_{coord}}{J_{iso} - J_{pool}} \tag{12}$$

Formula (13) expresses the committed depth as the average number of blocks online. Formula (14) converts the sum of daily negative F_t values into net east-west energy in GWh. Absolute transport energy is also reported because reverse flow may cause the total exchange to exceed the daily net value.

$$\bar{N}_{on} = \frac{1}{|\mathcal{T}|}\sum_{t\in\mathcal{T}}\sum_{g\in\mathcal{G}} u_{g,t} \tag{13}$$

$$E_{E\to W} = -\frac{1}{1000}\sum_{t\in\mathcal{T}} F_t \quad \text{when} \sum_{t} F_t < 0 \tag{14}$$

5. Computational Implementation and Experimental Scheme

Intlinprog library implementation . A standalone Python refactoring using SciPy and HiGHS libraries validated target values, integrity, regional balancing, generation limits, ramping capability, shortest time logic, switching limits, and load reduction residuals [20][21]. This standalone path was used only for numerical validation and not as a different scheduling method.

Under the three architectures in Table 1, 24-hour independent solutions were performed for each of the 19 operating dates. All solutions used the same initial block state, output, demand, calibration cost, generation limit, ramp limit, and minimum operating time values. Results were accepted only if the regional power balance and all binary and intertemporal constraints met numerical tolerances.

This transmission capacity sensitivity analysis selected two representative dates for study. The case of May 5th has the highest coordinated economic value, while August 5th is a peak day of 8166 MW. The values of Fmax range from 0, 100, 200, 300, 349.6, 500, 750, 1000, and 5000 MW. This design reveals both the marginal economic response and the critical point at which additional transmission capacity no longer alters power dispatch or commitment.

Table 4 summarizes the controlled experimental design and acceptance checks used in this paper.

Table 4. Controlled experimental design.

element	treat
Requirements and initial state	The same in all three frames
Power generation combination and cost	Completely identical
Time limit	The same UC equation
Changing experimental factors	Limited to cumulative redemption amount
Main output	Goals, communication, commitment, transformation, technology and energy
Acceptance inspection	Integrity, balance, constraints, slope, shortest time, zero fallout

Table 4 clearly illustrates the causal relationship: the reported harmonization values are not generated by changing the data or equations, but by allowing the same physical model to exchange limited power between the two regional portfolios.

6. Results

6.1 Total Economic and Operating Value

Table 5 presents the overall comparative results before analyzing daily fluctuations. This table takes into account economic, commitment, cyclical, and trading indicators, so no single indicator should be interpreted in isolation.

Table 5. Summary results of 19 business days.

index	isolated	coordination	partnership
Overall target (million CU)	97.759	97.094	96.987
Reduction (%) compared to separation	-	0.680	0.789
Average number of committed blocks	9.80	9.11	9.17
Start/Stop Transition	205	196	198
Absolute transaction volume (GWh)	0	105.85	142.48
Net energy from west to east (GWh)	0	-87.32	-139.02
Model load reduction (megawatt-hours)	0	0	0

The reconciliation model reduced the total objective by 664,835 units (CU) (0.680%) and utilized 86.17% of the available pool value. The remaining transfer constraint costs accounted for only 0.110% of the reconciliation objective. Reconciliation also reduced the average commitment by 7.09%, reduced the number of transitions by 4.39%, and achieved load-free reductions in every simulation hour.

Figure 3 compares the daily targets under the three frameworks. The horizontal axis is arranged chronologically for 19 operating days, while the vertical axis reports the daily targets in millions of CUs.

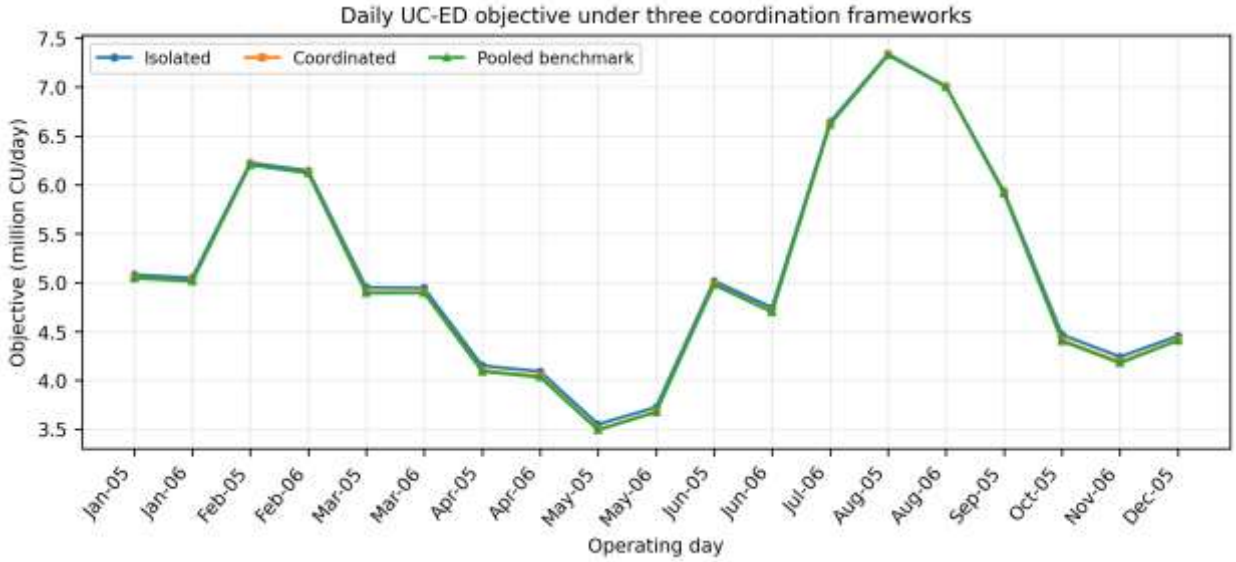


Figure 3. Daily UC-ED targets under individual scheduling, coordinated scheduling, and centralized scheduling.

Figure 3 shows that the coordinated merging curve and the combined curve are lower than the individual curves on every day. The vertical distance is greatest under low and medium load conditions; while during the summer peak season, the vertical distance is smaller, at which point both regions need to deploy a large number of local fleets.

Figure 4 converts the objective differences in Figure 3 into a percentage reduction relative to individual shifts. The dashed line represents the 19-day average.

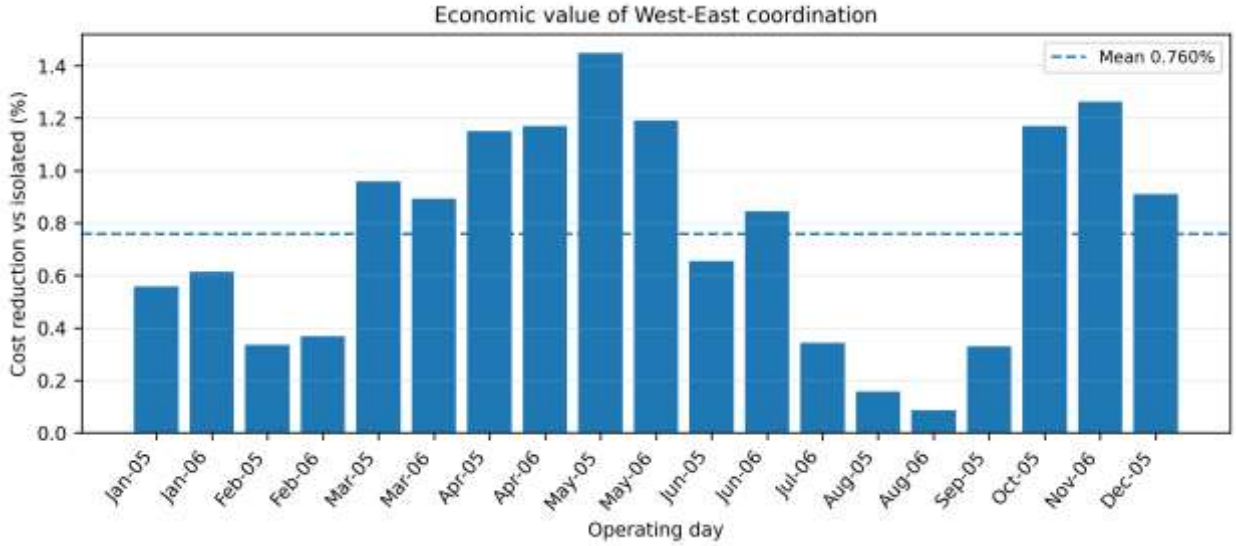


Figure 4. Daily target reduction achieved through coordinated scheduling between East and West.

In Figure 4, the daily decline ranged from 0.086% to 1.448%, with an average of 0.760%. The highest value occurred on May 5th, while the smallest decline was on August 6th. This volatility suggests that the value of coordination depends on regional cost separation, committed flexibility, and available allocation margins, rather than just demand.

6.2 Trading Direction and Daily Fluctuations

Figure 5 shows the daily net energy exchange. Positive values indicate energy flow from west to east, and negative values indicate energy flow from east to west. The notation conventions are the same as in equation (14).

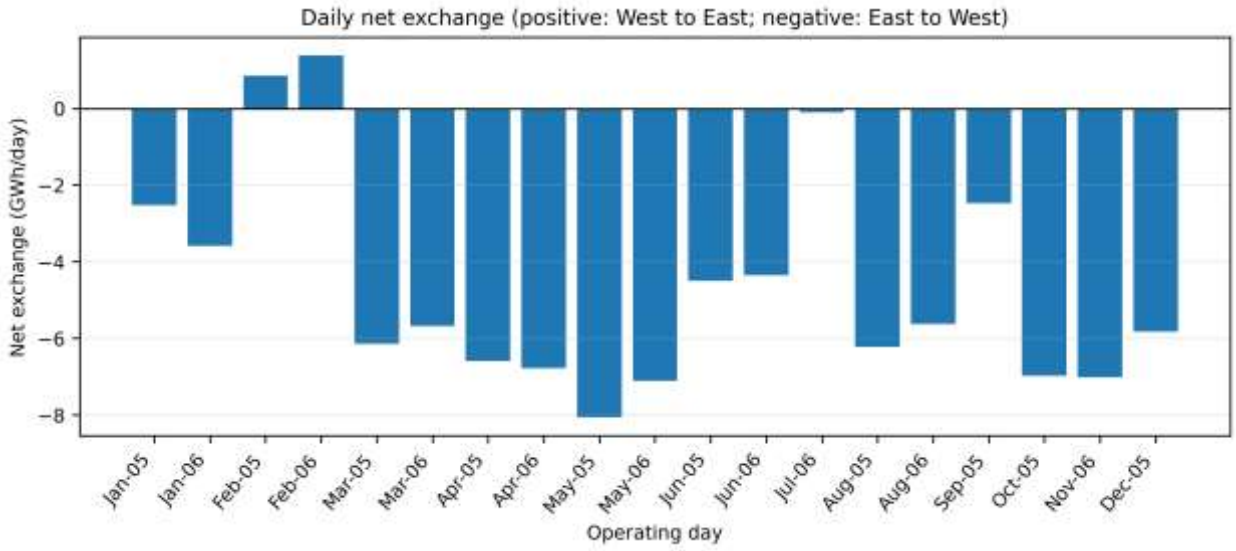


Figure 5. Daily net exchange volume under coordinated scheduling; negative values represent east-west energy.

The coordination model arranged net energy transport from east to west for 17 out of 19 days, and net energy transport from west to east for the two cases in February. The total net transport from east to west was 87.32 GWh, while the absolute transport was 105.85 GWh. The difference between the net and absolute values confirms that there was reverse energy transport across time periods on certain dates; net transport alone cannot reflect the total utilization of the corridor.

Table 6 provides the full numerical evidence behind Figures 3-5. It lists each run date, rather than just selecting favorable cases.

Table 6. Complete 19-day coordinated work schedule certificate.

date	Peak megawatts	Plasma. MCU	Coordination M CU	reduce%	Net Energy → Energy (GWh)	Average block I/C	Time Limit
January 5	6,243	5.081	5.052	0.558	2.524	10.54/9.04	4
January 6	6,440	5.049	5.018	0.613	3.579	10.12/9.04	7
February 5	7,550	6.225	6.204	0.336	-0.854	12.00/11.00	0
February 6	7,400	6.146	6.123	0.367	-1.389	11.62/11.12	2
March 5	6,299	4.951	4.904	0.959	6.144	10.04/9.04	11
March 6	6,075	4.944	4.900	0.892	5.675	10.04/9.04	7
April 5	5,535	4.150	4.102	1.150	6.595	8.12/7.17	10
April 6	5,510	4.092	4.044	1.170	6.779	8.13/7.08	12
May 5	4,665	3.551	3.500	1.448	8.068	7.08/6.08	18
May 6	5,115	3.726	3.682	1.190	7.109	7.08/7.04	14
June 5	6,480	5.016	4.983	0.655	4.497	10.08/9.04	8
June 6	5,808	4.746	4.706	0.844	4.353	9.12/9.04	7
July 6	7,645	6.641	6.619	0.344	0.099	11.79/11.04	0
August 5	8,166	7.339	7.327	0.157	6.220	12.04/12.00	7
August 6	7,870	7.009	7.002	0.086	5.618	12.00/12.00	1
September 5	6,640	5.932	5.912	0.329	2.477	11.21/11.04	0
October 5	5,635	4.467	4.414	1.170	6.980	9.04/8.08	11
November 6	5,600	4.242	4.188	1.263	7.019	8.04/7.04	12
December 5	5,787	4.454	4.413	0.909	5.829	8.08/8.04	9

Table 6 confirms that the daily target values have all decreased. The table also shows that the direction of exchange rate changes and the duration of constraints vary depending on operating conditions. Therefore, this table is the primary audit basis for the daily reporting in this section.

6.3 Peak Days and Days with the Highest Value

Table 7 compares and analyzes the two selected representative cases in detail. The high-value case tests economic flexibility, while the peak case tests how to coordinate when most of the fleet is already occupied.

Table 7. Results of representative business days.

case	Isolated/coordinated MCU	reduce%	Net Energy → Energy (GWh)	Time Limit	Average block I/C
Date of highest value: May 5, 2025	3.551 / 3.500	1.448	8.068	18	7.08 / 6.08
Peak day: August 5, 2025	7.339 / 7.327	0.157	6.220	7	12.04 / 12.00

On May 5th, the coordination mechanism cancelled an average of about one block of commitments, and the exchange constraints lasted for 18 hours. On August 5th, due to system peaks requiring the most economical capacity, the number of commitments remained almost unchanged; however, the exchange mechanism still reduced the target capacity and maintained the constraints for 7 hours.

Figure 6 compares the demand in the eastern and western regions under peak-day coordinated power generation. Each regional power generation curve includes the local effects of optimized exchange.

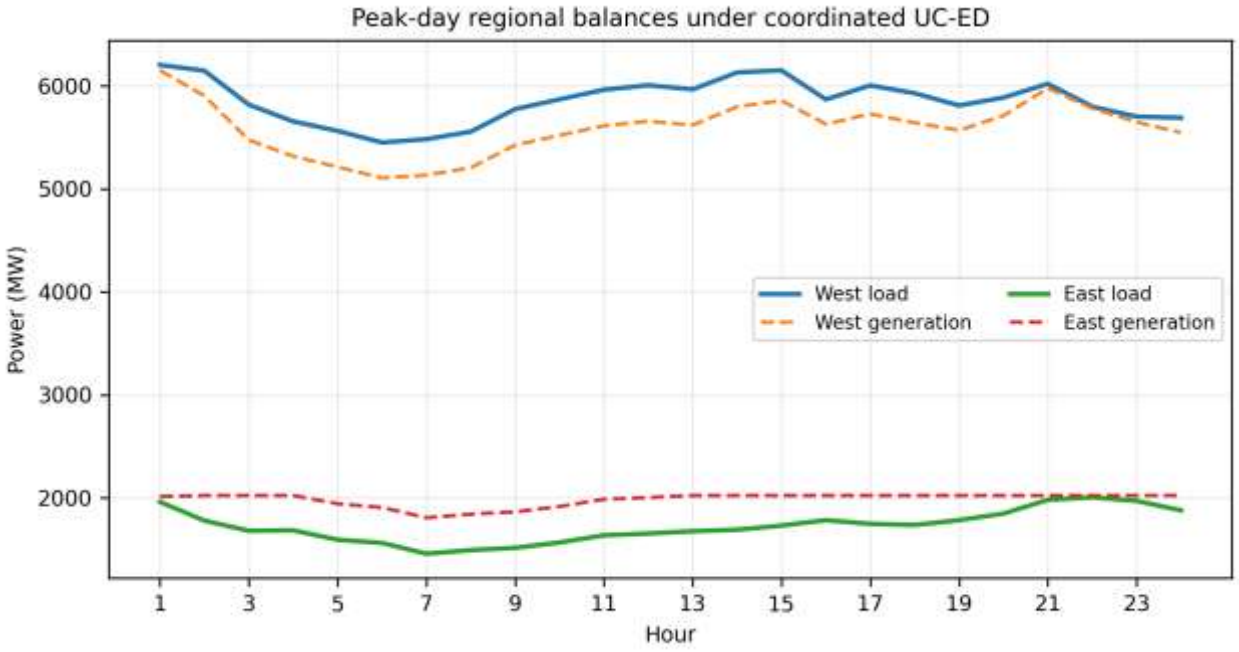


Figure 6. Regional demand and coordinated power generation on peak days.

Figure 6 shows that during most peak hours, power generation in the eastern region exceeds demand. The excess electricity is transmitted to the western region, thus reducing demand there. Therefore, the coordination scheme alters the location of power generation while maintaining overall hourly balance.

Figure 7 shows the corresponding hourly exchange rate. The dashed line represents ±349.6 MW, and negative values represent east-west support.

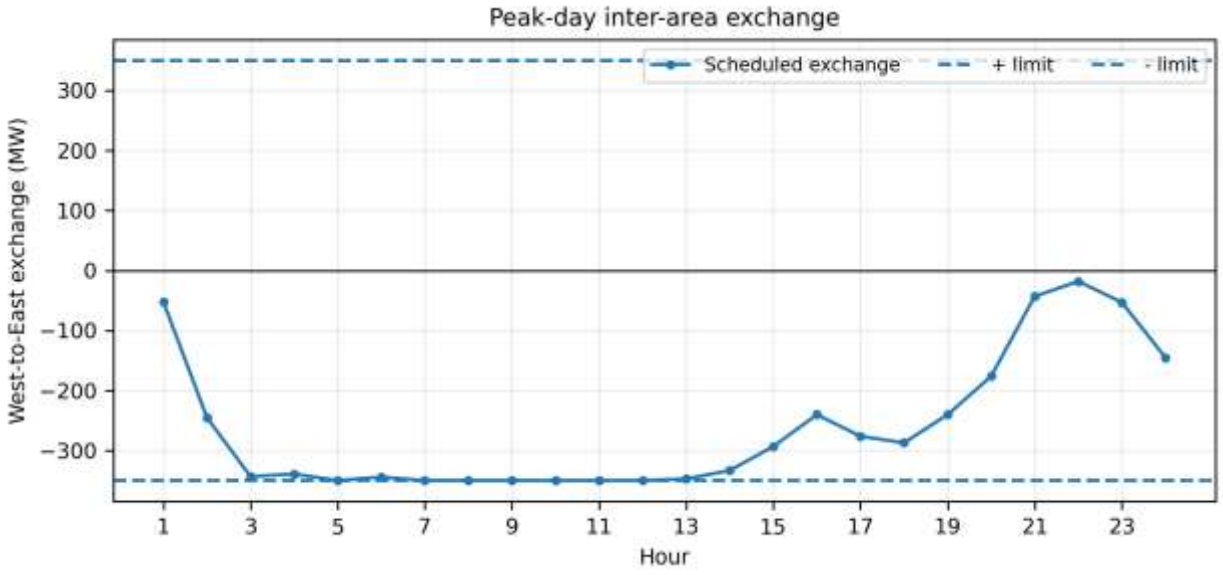


Figure 7. Peak daily total exchange volume and calibration transfer limits.

As shown in Figure 7, power exchange remained within east-west limits for up to seven hours, especially during periods of high load. Towards the end, power flow approached zero as regional demand and commitments changed. This result explains why national power capacity adequacy alone is insufficient to determine economic power generation plans: the availability and location of power generation facilities are also crucial.

Figure 8 shows the commitment matrix for the day with the highest value. Rows represent site blocks, columns represent hours, black cells indicate online status, and white cells indicate offline status.

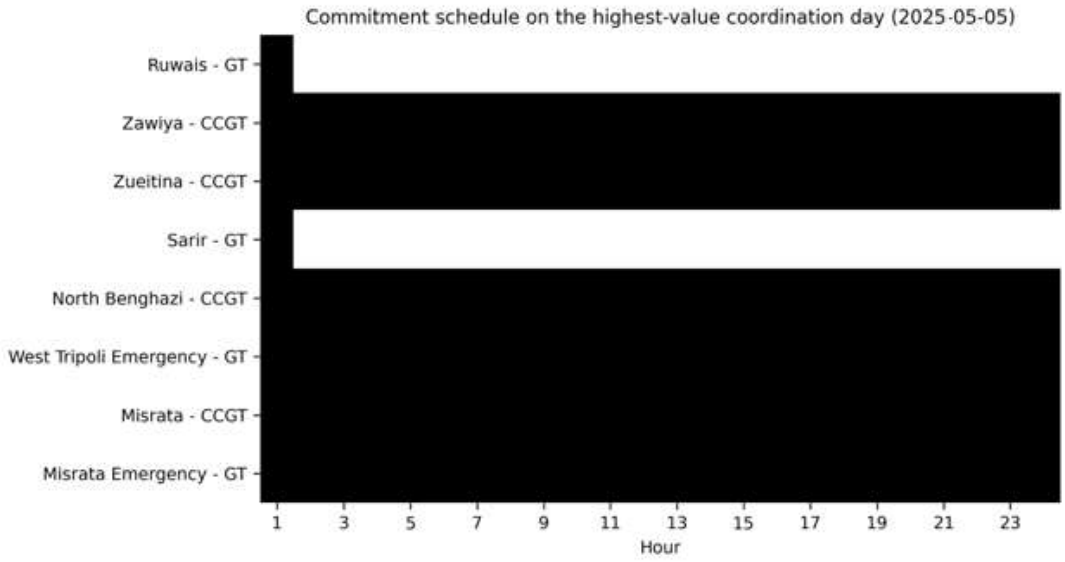


Figure 8. Coordination commitment plan for May 5, 2025 (the most valuable day).

The long horizontal bars in Figure 8 show that the coordination solution does not switch every hour. It selects a stable six-block core and retains the other blocks needed for the daily trajectory. The average number of committed blocks decreased from 7.08 to 6.08, while the total target value decreased by 1.448%.

6.4 Transfer Capability Sensitivity

Table 8 lists the complete nine-point sensitivity sequences for two representative dates. When the capacity is zero, the exchange capacity is fixed at zero, so the mathematical boundary is valid for all 24 hours; this should be interpreted as isolated operation rather than congestion of the physical lines.

Table 8. Transferability sensitivity of the highest and peak dates.

Limited megawatts	May reduction percentage	May E→W GWh	May	August decline	August E→W GWh	August at the border
0	0.000	-0.000	twenty four	0.000	-0.000	twenty four
100	0.453	2.222	twenty three	0.099	2.120	20
200	0.918	4.522	twenty three	0.145	4.087	18
300	1.304	7.132	20	0.156	5.662	11
349.6	1.448	8.068	18	0.157	6.220	7
500	1.620	9.874	9	0.158	6.841	1
750	1.634	10.715	0	0.158	6.849	0
1000	1.634	10.715	0	0.158	6.849	0
5000	1.634	10.715	0	0.158	6.849	0

Table 8 illustrates the monotonous but rapidly saturating response. At 349.6 MW, the May operating condition captured 88.6% of its maximum sensitivity, while the peak operating condition captured over 99% of its maximum value. Therefore, the marginal transfer value is strongly dependent on the operating condition.

Figure 9 visualizes the target reduction column in Table 8. The two curves use the same horizontal scale, allowing for a direct comparison of their different saturation behaviors.

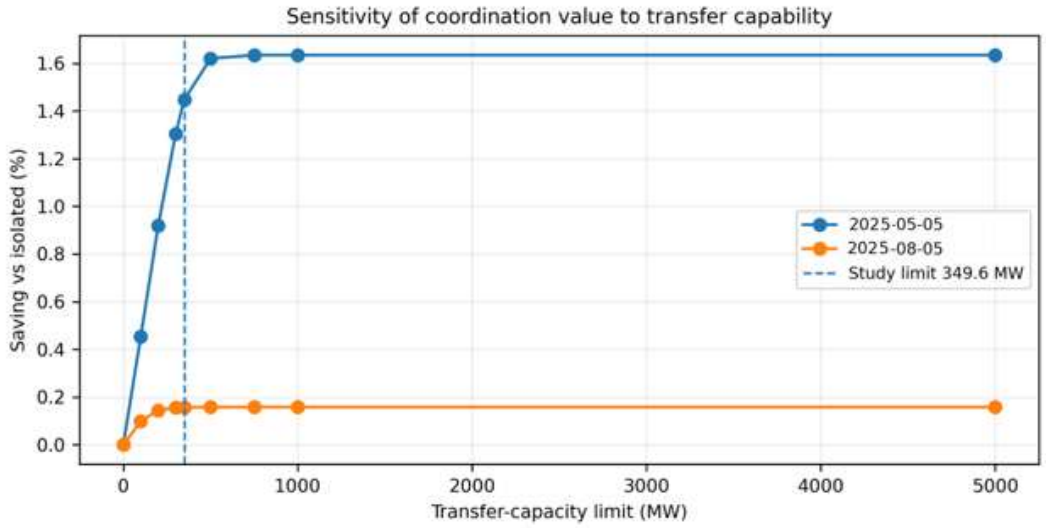


Figure 9. The goal is to reduce sensitivity to total transfer capacity.

The curve rose rapidly in May, reaching 500-750 MW, before settling at 1.634%. The peak curve in August was much flatter, essentially saturating at 500 MW, reaching 0.158%. Therefore, larger corridors are only valuable when regional commitments and marginal cost differences create opportunities for economic substitution.

Figure 10 shows the peak day transmission capacity duration curves, ranked by number. It complements Table 8, showing how many hours of transmission demand exceeded each capacity level.

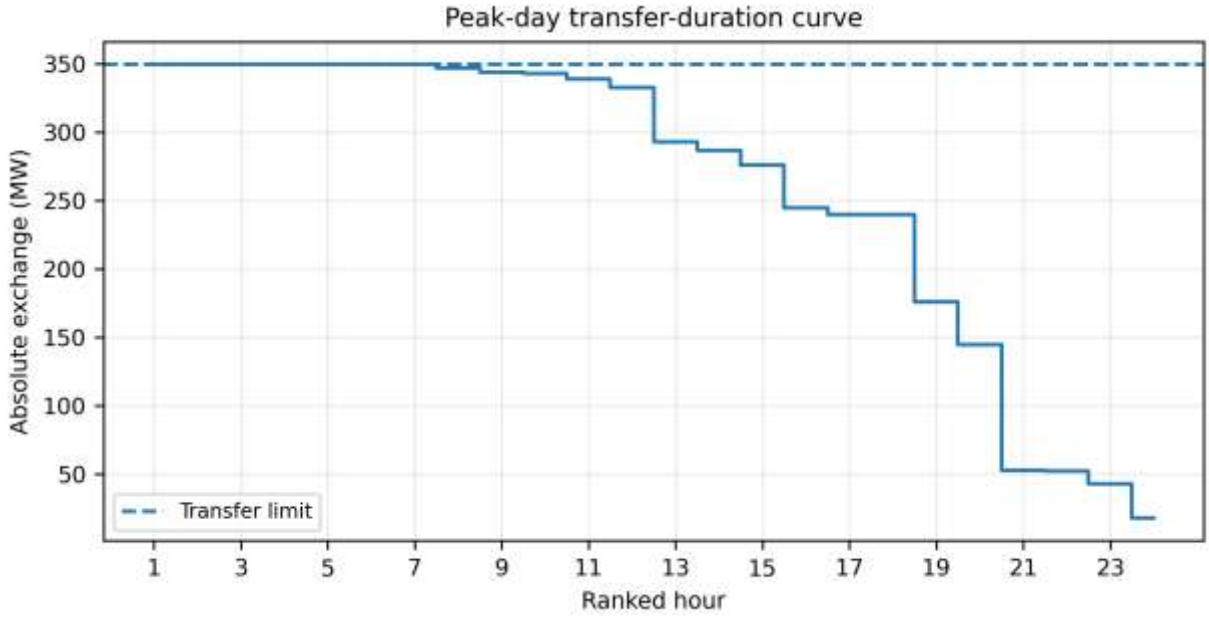


Figure 10. Ranking of peak day transfer capacity demand and duration.

Figure 10 ranks the absolute transmission demand on peak days from highest to lowest hourly demand. The horizontal line of 349.6 MW intersects the duration curve at 7 hours, consistent with Table 8. This duration perspective is useful because almost all the economic value of transmission capacity expansion can be realized by eliminating the constraints of a few peak periods.

6.5 Commitment, Cycle, and Technology Allocation

Figure 11 compares the average depth of commitment across the three frameworks. Commitment is an operational outcome, not an independent objective; it must be interpreted in conjunction with costs, transition, and service needs.

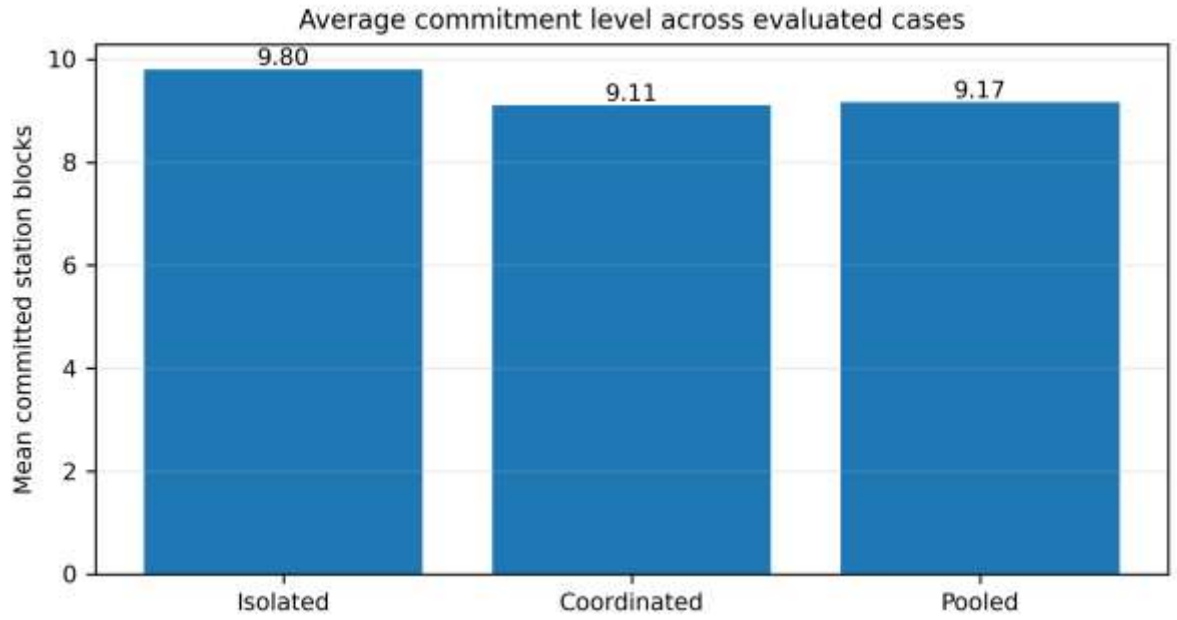


Figure 11. Average number of committed site blocks in isolated scheduling, coordinated scheduling, and centralized scheduling.

The coordination mechanism reduced the average number of committed blocks from 9.80 to 9.11. Despite the lower target value, the average number of committed blocks in the merge baseline was slightly higher at 9.17. This result indicates that minimum cost and minimum number of online blocks are related but not identical objectives; different commitment strategies can achieve more economical scheduling.

Figure 12 shows the overall situation of the start/stop transition. This chart is designed to ensure that the cyclical impact of cost improvements is not overlooked when interpreting cost improvements.

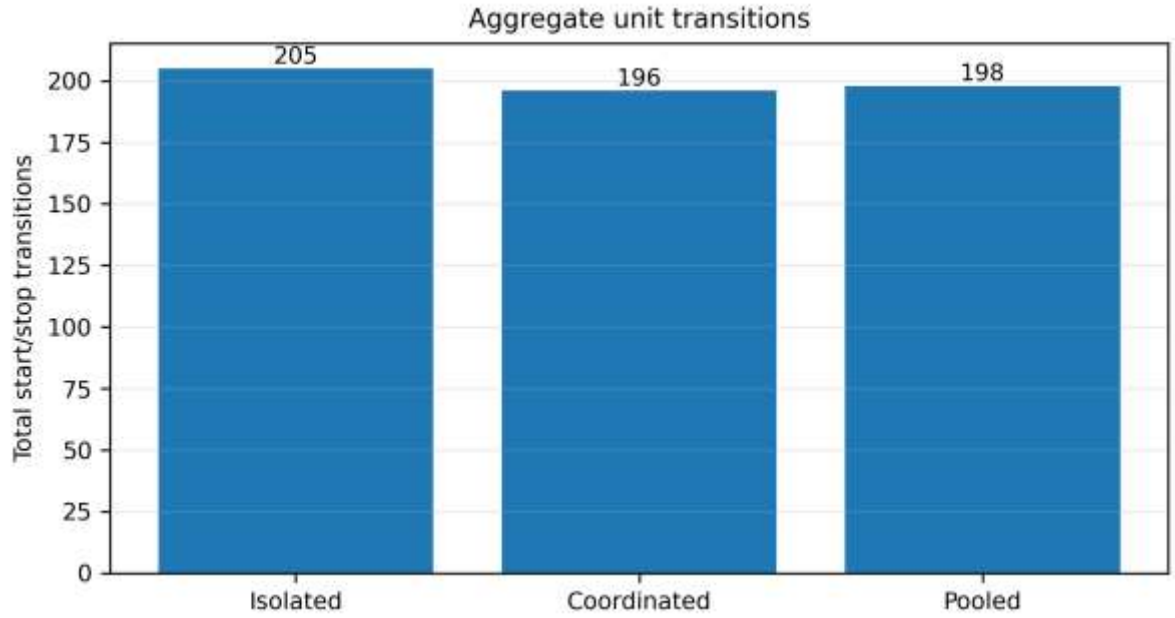


Figure 12. Total startup and shutdown conversions under the three frameworks.

The collaborative operation recorded 196 transformations, compared to 205 for the standalone operation and 198 for the merged baseline. The reduction in transformation count is not significant, but it aligns with the shallower commitment depth. More importantly, the results indicate that the collaborative solution does not achieve cost reductions by introducing excessive loops.

Figure 13 compares the peak daily power consumption for different technology categories. The bar chart shows the daily power consumption allocated to each technology category, not the device capacity.

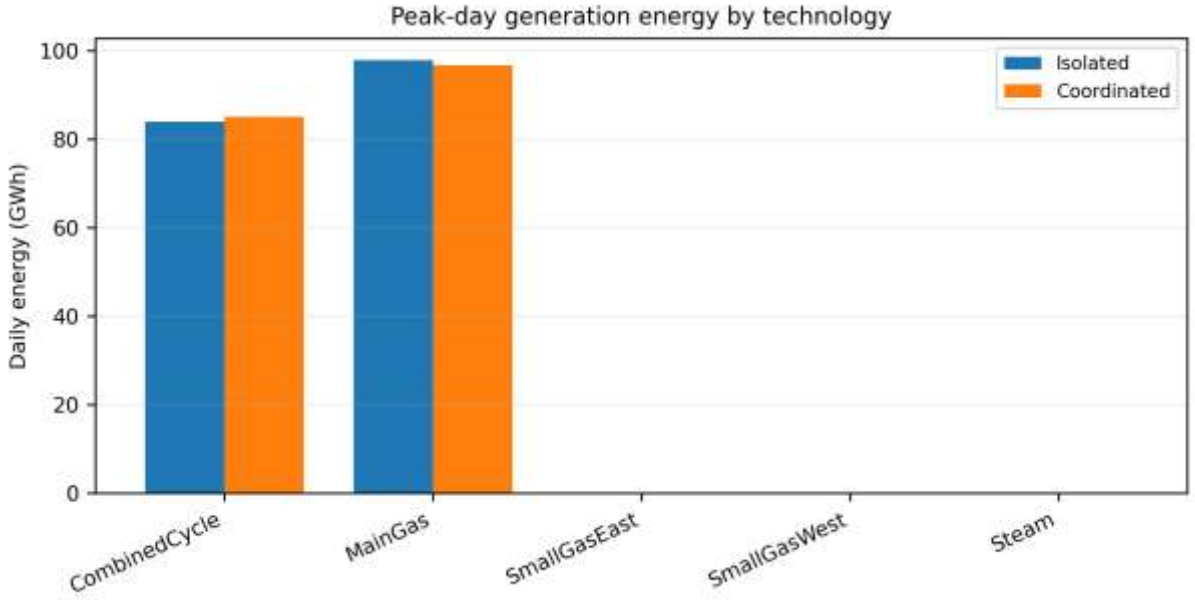


Figure 13. Peak daily power generation of various technologies under isolated dispatch and coordinated dispatch.

On peak electricity days, coordinated measures will increase combined cycle power generation from 83.94 GWh to 85.14 GWh, while reducing main gas turbine power generation by the same amount, while small gas and steam turbines remain unused in the calibration scheme adopted. This change is small relative to total daily power generation and is consistent with the target reduction of 0.157% on peak days.

7. Project Discussion and Implementation Recommendations

The study distinguishes three often-confused concepts: national sufficiency, regional economic alternatives, and physical network security. This model demonstrates that bounded area switching alters the economic inputs and scheduling of the adopted combinations. The model does not assign switching to specific loops; detailed implementation should use the official 400/220/66 kV node model and validated branch and transformer parameters.

The predominantly east-west energy transport direction is not a fixed operating rule, but rather the result of the combined effects of the 2025 demand curve, initial conditions, and a calibrated relative cost ranking. In the two cases in February, the energy transport direction reversed, demonstrating that the optimized system can flexibly arrange west-to-east energy supply according to regional economic needs.

The transmission sensitivity analysis results provide practical guidance for planning. The current study limit of 349.6 MW covers most of the economic value in both case studies, but there is still an additional revenue of approximately 750 MW on high-value days. Therefore, detailed grid studies should prioritize the time periods and locations where this residual value can be generated, rather than assuming that each increase in transmission capacity will bring the same annual revenue.

To facilitate implementation, the recommended workflow is as follows: (1) Import the latest demand forecast and unit status; (2) Load the approved unit and regional exchange parameters; (3) Solve isolated and coordinated cases in parallel; (4) Present the target, exchange, commitment, conversion and constraint margin differences to the dispatcher; (5) Validate the proposed contingency plan in the official AC and exchange models; (6)

This paper uses comparative cost units to ensure consistent evaluation of the coordination mechanism. Before implementing financial or scheduling plans, the calibrated relative costs should be replaced with audited heat rates, fuel prices, no-load, start-up, and shutdown data. This replacement will not alter the equations or experimental design.

8. Conclusion

This paper constructs a controlled dual-region unified capacity dispatch (UC-ED) model for the Libyan power system and quantifies the economic value of bounded east-west coordination. All models use the same 19 authorized operating days, 25 power station periods, demand, initial state, time constraints, and cost coefficients; only the total exchange limit varies.

Throughout the sample, coordinated scheduling reduced the total target from 97.759 million CUs to 97.094 million CUs, achieving 86.17% of the centralized economic value, reducing the average committed volume from 9.80 blocks to 9.11 blocks, and decreasing the number of transitions from 205 to 196. Coordinated scheduling transferred 105.85 GWh of absolute power and 87.32 GWh of net power from east to west, and the model predicted no load shedding.

These detailed case studies explain why average outcomes cannot be represented by a single transfer value. The highest-value day achieved a 1.448% emissions reduction and continued to benefit until approximately 750 MW; while the peak day of 8166 MW achieved only a 0.157% emissions reduction and was almost fully saturated at 500 MW. Therefore, the main conclusion is that the value of interregional capacity depends on the flexibility and cost separation of regional commitments, not just demand or installed capacity.

This study provides a repeatable economic screening phase for national coordination. The next recommended step is to apply the same commitment and sensitivity logic to official node AC grids, verified cell-level cost data, and approved converter policies to translate economic signals into detailed operational recommendations.

refer to

[1] AJ Wood, BF Wollenberg and GB Sheblé , Power Generation, Operation and Control, 3rd ed. Hoboken, NJ: Wiley, 2014.

[2] M. Carrión and JM Arroyo, “Computationally efficient mixed-integer linear formulas for cogeneration unit combination problems”, IEEE Transactions on Power Systems, Vol. 21, No. 3, pp. 1371-1378, August 2006, doi : 10.1109/TPWTPWRS.

[3] J. Ostrowski, MF Anjos and A. Vannelli, “A compact mixed-integer linear programming formula for the unit combination problem”, IEEE Transactions on Power Systems, Vol. 27, No. 1, pp. 39-46, February 2012, doi : 10.1109/TPWRS.2011.8.

[4] G. Morales-España, JM Latorre and A. Ramos, “Compact MILP formula for cogeneration unit combination problem”, IEEE Transactions on Power Systems, Vol. 28, No. 4, pp. 4897-4908, November 2013, doi 20120132513.17313.201313135313020130213021302130213020131 3025.130213 .

[5] G. Morales-España, JM Latorre and A. Ramos, “Compact MILP formulas for start-up and shutdown ramps in unit combinations”, IEEE Transactions on Power Systems, Vol. 28, No. 2, pp. 1288-1296, May 2013, doi : 10.110292.1232.32312020123123020123123123023125, 20123235, 13892.1231235, 13292.1231235

[6] B. Knueven, J. Ostrowski and J.-P. Watson, “A mixed integer programming formula for the unit combination problem”, INFORMS J. Comput ., Vol. 32, No. 4, pp. 857-876, 2020, doi : 10.1287/ijoc.2019.09401.

[7] RH Wuijts , M. van den Akker and M. van den Broek, “The impact of modeling choice in the unity commitment problem”, Energy Systems, Vol. 15, pp. 1-63, 2024, doi : 10.1007/s12667-023-00564-5.

[8] RR Shoults, SK Chang, S. Helmick and WM Grady, “Practical approach to unit combination, economic dispatch and cost-saving allocation for multi-regional power pool operation with import and export constraints”, IEEE Trans. Power App. Syst., Vol. PAS-99, No. 2, pp. 625-635, 1980, doi : 10.1109/TPAS.1980.319654.

[9] A. Papavasiliou and SS Oren, “Multi-regional stochastic unit combinations with high wind power penetration in transmission-constrained networks”, Operations Research, Vol. 61, No. 3, pp. 578-592, 2013, doi : 10.1287/opre.2013.1174.

[10] MJ Mokarram , “Robust and efficient parallel processes for coordinating multi-regional economic scheduling problems in the presence of uncertainty”, IET Gener. Transm. Distrib ., Vol. 13, No. 18, pp. 4197-4205, 2019, doi : 10.1049/iet-gtd.2019.199.10.1049/i-gtd.

[11] X. Zheng, H. Chen, Y. Xu, F. Shen and Z. Liang, “A Global Solution Method for Distributed Multi-Region SCUC and Economical Allocation Based on MILP Value Function”, IET Gener. Transm. Distrib ., Vol. 14, No. 16, pp. 3230-3240, doi : 10.1049/iet-gtd.2020.0438.

[12] C. Yingvivatanapong , W.-J. Lee and E. Liu, “Multi-regional generation dispatch in competitive markets”, IEEE Transactions on Power Systems, Vol. 23, No. 1, pp. 196-203, February 2008, doi : 10.1109/TPWTPRS.RS.

[13] A. Aharwar , R. Naresh, V. Sharma and V. Kumar, “Transmission system unit combination problem, models and methods: a review”, Electric Power System Research, Vol. 223, No. 109671, 2023, doi : 10.1016/j.epsr.2023.109671.

[14] C. O'Malley, P. de Mars, L. Badesa and G. Strbac , “Reinforcement learning and mixed integer programming for power plant dispatching in low-carbon systems: comparison and hybridization ,” Applied Energy, Vol. 349, No. 121659, 2023, doi : 10.1016/j.2120123.120212020209.129.2025.12320259.2025.12025.12025.125259.2025.12025.2025.125025.2025.125259.1259.2025.125209.1259.

[15] Á. S. Xavier, F. Qiu and S. Ahmed, “Learning to solve large-scale safety-constrained unit combination problems”, INFORMS J. Comput ., Vol. 33, No. 2, pp. 739-756, 2021, doi : 10.1287/ijoc.2020.0976.

[16] L.

[17] M. Liu, X. Kong, K. Xiong, J. Wang and Q. Lin, “Multiscale spacetime converter: a novel model simplification method for day-ahead safety-constrained unit combination”, Applied Energy, Vol. 380, No. 124963, 2025, doi : 10.1016/j.10.1920.j.

[18] A. Ihbal and A. Khalleefah , “Predicting short-term peak load demand in the Libyan power grid using a multiple regression model”, Journal of Pure and Applied Sciences, Vol. 22, No. 3, pp. 124-128, 2023, doi : 10.51984/ jopas.v2i3 .

[19] General Electricity Company of Libya, “Authorized State Operation Records for Academic Unit Combination and Economic Dispatch Studies”, Internal Operation Records, 2025, Unpublished.

[20] P. Virtanen et al., “SciPy 1.0: Basic Algorithms for Scientific Computing in Python”, Natural Methods, Vol. 17, pp. 261-272, 2020, doi : 10.1038/s41592-019-0686-2.

[21] Q. Huangfu and JAJ Hall, “Parallelization Dual Modified Simplex Method”, Mathematical Programming and Computation , Vol. 10, No. 1, pp. 119-142, 2018, doi : 10.1007/s12532-017-0130-5.